 doi:10.20944/preprints202011.0691.v1

Huanglian Decoction suppresses the growth of hepatocellular carcinoma cells by reducing CCNB1 expression

Min Li[1], Hua Shang[1], Tao Wang[2], Shuiqing Yang[3], Lei Li[3,4#]

1. Department of Gastroenterology, Zibo Central Hospital, Zibo, Shandong 255036, China.
2. Department of General Surgery, Zibo Central Hospital, Zibo, Shandong 255036, China.
3. School of Biological Science and Medical Engineering, Beihang University, Beijing 100191, China.
4. Department of Pathology, Dunedin School of Medicine, University of Otago, Dunedin 9054, New Zealand.

[#]Corresponding author:
Lei Li, School of Biological Science and Medical Engineering, Beihang University, Beijing 100191, China; Department of Pathology, Dunedin School of Medicine, University of Otago, Dunedin 9054, New Zealand
Email: wshililei@buaa.edu.cn.

Abstract

Background: Hepatocellular carcinoma (HCC) is one of the most prevalent cancers in human populations worldwide. Conversely, Huanglian Decoction is one of the most important Chinese medicine formulas, with the potential to treat cancer.

Methods: To identify differentially expressed genes (DEG), we herein downloaded gene expression profile data from the TCGA (TCGA-LIHC) and GEO (GSE45436) databases. We obtained phytochemicals of the four constituent herbs of Huanglian Decoction from the traditional Chinese medicine systems pharmacology database and analysis platform (TCMSP). We also established a regulatory network of DEG and their drug target genes and subsequently analyzed key genes using bioinformatic approaches. Furthermore, we explored the effect of Huanglian Decoction by conducting in *vitro* experiments so as to verify the prediction. In particular, the CCNB1 gene was knockdown to verify the primary target of this Decoction.

Results: Based on the results of network pharmacological analysis, we revealed that there are 5 bioactive compounds in Huanglian Decoction acting on HCC. In addition, our findings confirmed that CCNB1 was the primary key gene, which can be highly expressed in tumors and was significantly associated with a worse prognosis ($P = 0.002$) according to PPI network analysis of the target genes of these five compounds, as well as expression and prognosis analyses in tumors. We also noted that CCNB1 can be used as an independent prognostic indicator of HCC ($P < 0.01$). Moreover, in *vitro* experimental results demonstrate that Huanglian Decoction can significantly inhibit the growth, migration, and invasion of HCC cells. Finally, further analysis showed that this Decoction may inhibit the growth of HCC cells by down-regulating the expression level of CCNB1.

Keywords: Huanglian Decoction (Coptidis Rhizoma, Zingiberis Rhizoma, Folium Artemisiae Argyi, Mume Fructus); Hepatocellular carcinoma; TCGA; GEO.

 doi:10.20944/preprints202011.0691.v1

Running Title: Effect of Huanglian Decoction on HCC

1. Introduction

Hepatocellular carcinoma (HCC) is the most frequent primary malignancy of the liver and the third leading cause of cancer mortality worldwide [1-3]. Current treatment options for liver cancer primarily include surgery, local treatment, biological treatment, and other different methods. Recently, molecular targeted therapy has been used to treat patients with advanced liver cancer to a certain extent, but because targeted drugs are relatively expensive and carry side effects, they have not been fully utilized [4-6]. In the past few years, there has been growing research attention in traditional Chinese medicine (TCM). Previous studies have been established that TCM can improve the clinical symptoms of patients, especially for those with advanced liver cancer by prolonging their survival period, and also the price is relatively cheap. In particular, TCM formulation contains a variety of chemical components that act on multiple targets and diseases [7-9]. However, the complexity and diversity of traditional Chinese medicine components have made our understanding of the specific molecular mechanisms of Chinese medicine are still largely unknown. This, therefore, limits the development of Chinese medicine. Nevertheless, the recent development of computer technology has allowed us to analyze the components of these medicines using computers and also systematically analyze their effects on diseases through network pharmacology, which has greatly promoted our understanding of the molecular network of Chinese medicines and their nature [10-12].

Huanglian Decoction is one of the classical Chinese medicine formulas, which has the effect of clearing heat and treating abdominal pain [13-15]. This formulation was originally recorded in the classic Chinese medicine book “Treatise on Febrile Diseases” (Chinese name: Shanghan Lun). In this study, we obtained the formulas of Huanglian Decoction from the ancient Chinese medicine book (Sheng Ji Zong Lu), which is one of the most classic recipes. The formula consists of four Chinese herbal medicines, namely, Coptidis Rhizoma, Zingiberis Rhizoma, Folium Artemisiae Argyi, and Mume

Preprints (www.preprints.org) | NOT PEER-REVIEWED | Posted: 27 November 2020 doi:10.20944/preprints202011.0691.v1

Fructus. In addition, this Decoction plays a pivotal role in the field of TCM due to its various values such as treating colds, white diarrhea, and abdominal pain [16-18]. In some Asia-Pacific regions, this Decoction is used as an auxiliary medicine for the treatment of liver cancer in folk. However, very few studies have investigated the treatment of HCC with this Decoction. Thus, in this respect, we herein aimed to explore and prove the therapeutic potential of Huanglian Decoction for HCC treatment.

In this work, we first identified the main target of Huanglian Decoction for liver cancer using network pharmacology and bioinformatics analysis. We then verified that this Decoction can inhibit the growth of HCC cells through in *vitro* experiments. Additionally, by knocking down the expression of CCNB1 protein in HCC cells, we confirmed that this Decoction mainly regulates HCC cells by inhibiting the expression of CCNB1. The detailed flow chart of this study is depicted in Fig. 1. Altogether, this study provides novel insights into the mechanism of Huanglian Decoction treatment for HCC.

2. Materials and methods

2.1 Data collection and cell culture

For this study, we downloaded the gene expression profile data of HCC patients from the TCGA database (https://portal.gdc.cancer.gov/). This dataset includes 347 tumors and 50 non-tumor samples. GEO (https://www.ncbi.nlm.nih.gov/geo/) is a public functional genomics data repository. The GSE45436 dataset contained 93 HCC tissue samples and 41 non-cancerous samples. We retrieved data from publicly available databases, hence it was not applicable for additional ethical approval. Then, we selected PLC/PRF/5 and HepG2 cells for the following experiments. Specifically, cells were purchased from the Chinese National Infrastructure of Cell Line Resource (NICR). The culture media was DMEM (Thermo Fisher Scientific, Waltham, MA), supplemented with 10% FBS. Finally, the cells were placed in an incubator (37 °C; 5% CO^2) as previously described.

2.2 Identification of DEGs

Here, we screened DEGs between HCC and non-cancerous samples using the "limma"

Preprints (www.preprints.org) | NOT PEER-REVIEWED | Posted: 27 November 2020 doi:10.20944/preprints202011.0691.v1

R package. The log_2FC (fold change) > 1 or < -1 and adj. *P*-values < 0.05 were considered statistically significant. To identify the differential genes shared by TCGA and GEO databases, we used TCGA data in the experimental group, while that of GEO was applied in the verification group. Afterward, the data results of the intersections were obtained and visualized using an online website (http://bioinformatics.psb.ugent.be/webtools/Venn/).

2.3 Identification and screening of bioactive components

For this experiment, we retrieved all phytochemicals of the four components of Huanglian Decoction from the Traditional Chinese Medicine System Pharmacology Database and Analysis Platform (TCMSP) (http://tcmspw.com/tcmsp.php). Based on the standards recommended by the TCMSP, we selected an oral bioavailability (OB) index ≥ 30% and drug-likeness (DL) index ≥ 0.18 to determine the pharmacological properties of the compound. Notably, compounds that meet all these criteria were considered biologically active ingredients [19-21].

2.4 Construction of the network

To comprehensively understand the molecular mechanisms of Huanglian Decoction, we collectively analyzed DEGs and active ingredients of the drug. Using Cytoscape version 3.7.2, we constructed Huanglian Decoction-compound, compound-target genes, and target gene-disease networks [22-24]. In addition, to further understand the relationship between target genes, we constructed a protein-protein interaction (PPI) network according to the information retrieved from the Search Tool for the Retrieval of Interacting Genes (STRING; https://string-db.org/) online database.

2.5 Prognostic analysis of key genes

Key genes in the network were extracted, and survival analyses were performed using R software ("survival" packages) to identify genes associated with prognosis, followed by univariate and multivariate COX analyses of genes associated with prognosis.

2.6 Gene Set Enrichment Analyses

To explore the potential molecular mechanisms of key genes, we performed a Gene Set Enrichment Analysis (GSEA) using the GSEA software version 4.0.3. The number of random sample permutations was set at 1000, while the significance threshold was set at $P < 0.05$ [25-28].

Preprints (www.preprints.org) | NOT PEER-REVIEWED | Posted: 27 November 2020 doi:10.20944/preprints202011.0691.v1

2.7 Preparation of Huanglian Decoction aqueous extract

The formula of Huanglian Decoction used in this study is different from the previous one. This formulation comprised of 50 grams of Coptidis Rhizoma, Zingiberis Rhizoma (25 grams), Folium Artemisiae Argyi (25 grams), and Mume Fructus (10 grams). All the above herbs were acquired from a Chinese TRT pharmacy. Briefly, to begin with, mix all herbs, then boil them in 1000 mL of distilled water for 2 h, and eventually remove the supernatant. Subsequently, centrifuge supernatant at 8000 rpm for 30 min and repeat the whole procedure twice. Lastly, redissolve the precipitate with distilled water to 10 mg/ml.

2.8 Wound-healing and transwell invasion assay

For wound healing assay, we treated cells with different concentrations of Huanglian Decoction (50 and 100 μg/mL for PLC/PRF/5 cells, 150 and 300 μg/mL for HepG2 cells) and then analyzed wound healing [29-31]. On the other hand, for transwell invasion assay, we treated HCC cells (1×10^5 cells/well) under different conditions, then fixed them with 4% paraformaldehyde for 2 h, followed by staining the invaded cells with crystal violet solution for 30 min. Finally, we counted the stained cells under an optical microscope.

2.9 siRNA transfection

siRNA targeting CCNB1 (CCNB1-siRNA, GAAUUCUGCACUAGUUCAA), was designed and synthesized by Nanjing InvivoGene Biotechnology Co., Ltd (Nanjing, China). We then performed siRNA transfection when the cells reached 70 - 80% confluence using Lipofectamine 2000 (Invitrogen, USA) as per the manufacturer's instructions.

2.10 Cell apoptosis analysis

To identify apoptotic cells, HCC cells were treated under different conditions. Using an Annexin V-FITC Apoptosis Detection kit (Thermo Fisher Scientific, Waltham, MA) after 48 h, we performed Annexin V and PI staining. The cell apoptosis was detected using a flow cytometer (ACEA, NovoCyteTM).

2.11 Western blotting analysis

Here, HCC cells in the logarithmic phase were seeded in a 10 cm dish. When the cells

Preprints (www.preprints.org) | NOT PEER-REVIEWED | Posted: 27 November 2020 doi:10.20944/preprints202011.0691.v1

occupied 80% of the dish, cells were then treated with Huanglian Decoction for 24 h in a culture media containing 10% FBS. Then, the harvested cells were disrupted, and the protein concentration was determined using a dye-binding protein assay kit according to the manufacturer's instruction manual. After centrifugation for 30 min, the supernatants were collected for protein measurement. After immersing the samples in 95 °C water for 10 min, the proteins were separated using gel electrophoresis and transferred to a membrane. Thereafter, the membranes were incubated overnight at 4 °C with primary antibodies (Rabbit monoclonal [Y106] to Cyclin B1, ab32053, 1/30000 dilution, Abcam, USA), and then further incubated with secondary antibodies (Goat Anti-Rabbit IgG H&L (HRP), ab205718, 1/5000 dilution, Abcam, USA) and eventually visualized.

2.12 Statistical analysis

Based on three independent experiments, data are expressed as mean ± SEM. All statistical analyses were implemented using R software version 3.5.0 (R Foundation for Statistical Computing, Vienna, Austria) and GraphPad Prism version 8.0.1 (GraphPad Software Inc., USA). If not specified above, a level of $P < 0.05$ was considered statistically significant.

3. Results

3.1 Identification of DEGs in HCC

We conducted this study as illustrated in the flow chart (Figure 1). To identify the common DEGs in the TCGA and GEO datasets, we performed differential gene analysis on the two datasets. We identified a total of 7667 differentially expressed genes at the mRNA level in tumor tissues (n = 374) compared with normal tissues (n = 50) based on the analysis of the TCGA dataset (Figure 2A). On the other hand, we identified a total of 1299 differentially expressed genes at the mRNA level in tumor tissues (n = 93) compared with normal tissues (n = 41) according to the GEO dataset analysis (Figure 2B). In summary, these results show an overlap of 838 DEGs (Figure 2C), between the TCGA and GEO datasets.

3.2 Identification of bioactive compounds in Huanglian Decoction

The four main active ingredients in Huang Ren Tang are Coptidis Rhizoma, Zingiberis

Preprints (www.preprints.org) | NOT PEER-REVIEWED | Posted: 27 November 2020 doi:10.20944/preprints202011.0691.v1

Rhizoma, Folium Artemisiae Argyi, and Mume Fructus. We retrieved the main chemical constituents of the four components from the TCMSP analytical platform and selected OB ≥ 30% and DL index ≥ 0.18 so as to determine the druggability of the compounds. Overall, we identified 765 bioactive compounds of the four main herbs, which were reduced to 24 after deleting duplicates (Supplementary Table S1).

3.3 Huanglian Decoction network analysis and PPI network analysis

To further understand the target genes of Huanglian Decoction, we constructed a regulatory network. First, the DEGs of disease and the target gene of Huanglian Decoction were subjected to intersection analysis, and 19 common genes were found (Figure 3A; Supplementary Table S2). Then, we constructed the Huanglian Decoction-compound, compound-target genes, and target gene-disease networks. As shown in Figure 3B, we uncovered 5 biologically active substances (Quercetin, Stigmasterol, beta-sitosterol, Worenine, and kaempferol) and 19 target genes (HSPB1, CCNB1, CYP1A2, BIRC5, NQO1, CDK1, FOS, CHEK1, TOP2A, E2F1, CHEK2, MAP2, SERPINE1, ADH1C, AKR1C3, IGFBP3, CYP3A4, MMP9, and PARP1). Finally, we constructed a protein interaction network for these 19 genes (Figure 3C) and screened the top 10 genes according to the number of nodes (Figure 3D).

3.4 Analysis of expression levels and survival of hub genes

In total, 10 genes were identified as hub genes. The survival analysis of the hub genes was evaluated using the Kaplan-Meier curve (Figure 4). Overall, we identified 7 genes that were significantly associated with prognosis (E2F1 ($P = 0.005$), MMP9 ($P = 0.014$), CDK1 (P = 1.36e-04), CHEK1 (P = 7.838e-04), CCNB1 (P = 0.002), BIRC5 (P = 4.06e-05), and TOP2A ($P = 0.001$)). We then analyzed the expression of these genes in tumors and normal tissues and found that most of them were highly expressed in tumors, except for FOS.

3.5 Identification of key prognostic genes in HCC

To further examine the role of key genes in prognosis, we herein conducted univariate and multivariate COX analyses of these genes. Among the results of the univariate COX analysis, we noted that CCNB1 (HR = 1.467, 95% CI = 1.252 - 1.719; $P < 0.001$), CDK1 (HR = 1.421, 95% CI = 1.207 - 1.673; $P < 0.001$), CHEK1 (HR = 1.919, 95% CI = 1.436 - 2.564; $P < 0.001$), E2F1 (HR = 1.134, 95% CI = 1.083 - 1.418; $P = 0.002$),

Preprints (www.preprints.org) | NOT PEER-REVIEWED | Posted: 27 November 2020 doi:10.20944/preprints202011.0691.v1

MMP9 (HR = 1.134, 95% CI = 1.023 - 1.256; *P* = 0.017), TOP2A (HR = 1.293, 95% CI = 1.133 - 1.476; *P* < 0.001), and BIRC5 (HR = 1.342, 95% CI = 1.171 - 1.538; *P* < 0.001) were all associated with poorer outcomes (Figure 5A). In the results of the multivariate COX analysis, we found that only CCNB1 (HR = 1.040, 95% CI = 1.011-1.070; *P* = 0.007) was associated with a worse prognosis (Figure 5B). These findings revealed that only CCNB1 can be used as an independent prognostic gene. Subsequently, we noticed that CCNB1 promotes tumor development (Figure 5C) and is associated with multiple biological pathways (Table 1; Figure 5D). Lastly, we performed GO (Supplementary Figure S1) and KEGG (Supplementary Figure S2) enrichment analyses on CCNB1 using R software.

3.6 Huanglian Decoction suppressed HCC cell growth in *vitro*

Here, we performed cell viability assays on liver cancer cells and the outcomes are depicted in Figure 6A. These findings demonstrate that Huanglian Decoction exhibited time- and dose-dependent effects on HCC cell viability. The IC50 value of Huanglian Decoction after 48 h treatment was about 100 μg/ml for PLC/PRF/5 and 200 μg/ml for HepG2 cells. Moreover, the results of apoptosis analysis indicated that this Decoction can induce apoptosis of both PLC/PRF/5 and HepG2 cells (Figure 6B). Interestingly, further analysis showed that this Decoction can reduce the migration and invasion activity of PLC/PRF/5 and HepG2 cells (Figure 6C; D).

3.7 Huanglian Decoction suppressed HCC cell growth in *vitro* by inhibiting the expression level of CCNB1 protein

To explore the potential mechanism of Huanglian Decoction on HCC cells, we first identified the protein level. Our results highlighted that this Decoction can reduce the CCNB1 protein expression levels in both PLC/PRF/5 and HepG2 cells. Furthermore, we noticed that after adding this Decoction (100 μg/ml for PLC/PRF/5 cells and 200 μg/ml for HepG2 cells) to the Si-CCNB1 group, the protein level did not change significantly (Figure 7A; B). Notably, the results of cell proliferation showed that the growth rate of cells was significantly reduced after transfection. Another important finding was that when this Decoction was added to the transfected cells, the growth rate of the cells did not change significantly (Figure 7C; D). Remarkably, the findings of

 doi:10.20944/preprints202011.0691.v1

cell apoptosis analysis revealed that inhibiting the expression of CCNB1 can promote apoptosis of both PLC/PRF/5 and HepG2 cells, whereas adding Huanglian Decoction to the cells after transfection did not significantly promote apoptosis (Figure 7E; F).

4. Discussion

In this work, we have found that Huanglian Decoction exhibits an effective therapeutic effect on HCC, primarily by inhibiting the expression level of CCNB1. Based on the analysis of TCGA and GEO databases, we identified DEGs in HCC. Subsequently, we also uncovered the main bioactive compounds associated with HCC in Huanglian Decoction and key target genes using network pharmacological analysis. Simultaneously, we further screened key genes through PPI network and survival analyses and ultimately, selected 7 genes (E2F1, MMP9, CDK1, CHEK1, CCNB1, BIRC5, and TOP2A) that meet the conditions. Afterward, we executed univariate and multivariate COX analyses on these 7 genes. The outcomes implied that CCNB1 can be used as an independent prognostic indicator. Another important finding is that CCNB1 is involved in the cell cycle, base excision repair, RNA degradation, spliceosome, oocyte meiosis, complement and coagulation cascades, drug metabolism - cytochrome P450, retinol metabolism, primary bile acid biosynthesis, and tryptophan metabolism signaling pathway of HCC (Figure 5D). Previous studies have established that the normal process of cell division occurs through the cell cycle. However, dysregulation of the cell cycle would result in sustained unscheduled cell growth, proliferation, and eventually a hallmark of cancer. Base excision repair is a key genomic maintenance pathway that possesses a tumor-suppressing effect. Therefore, CCNB1 may regulate the development of HCC through these pathways. We also established an in *vitro* experimental model. Our results show that Huanglian Decoction can inhibit the growth of HCC cells in *vitro*. Further analysis elucidated that this Decoction exhibited no obvious inhibitory ability on HCC cells (Si-CCNB1). Thus, we speculated that this Decoction might inhibit the growth of HCC cells by suppressing the expression of CCNB1. Collectively, these findings suggest that this formulation may have the potential to treat liver cancer.

 doi:10.20944/preprints202011.0691.v1

Multiple reports have highlighted that the Chinese medicine formula plays an essential role in the treatment of tumors. For instance, Ze-Qi-Tang (ZQT) can inhibit the growth of non-small cell lung cancer cells [32], whereas Jianpi Jiedu Decoction (JPJD) can inhibit the tumorigenesis, metastasis, and angiogenesis of colorectal cancer [33]. In addition, Huanglian Jiedu Decoction (HLJDD) can induce apoptosis and cell cycle arrest, as well as inhibit the migratory and invasive properties of HCC cells [34, 35]. These results further support the idea of the TCM formula as a potential agent of complementary and alternative treatment for cancer. Nonetheless, our literature search found that most of the TCM formulas related to Huanglian include Huanglian Jiedu, Huanglian-Wendan, and Huanglian-Renshen Decoctions, and thus there are paucities of studies on Huanglian Decoction. Interestingly, a recent article has reported that Huanglian Decoction possesses a certain therapeutic effect on diabetes, but the formula source of this Decoction is somewhat different from the formula in this work, so it may not have a reference value. However, it is important to note that the differences between different formulas and the potential medicinal value may be the next step to be explored. This is a critical area for future research that needs to be addressed.

CCNB2, also known as cyclin B2, is a member of the cyclin family. CCNB2 was reported to regulate the cell cycle by activating CDC2 kinase in eukaryotes, and inhibition of CCNB2 induced cell cycle arrest [36-38]. CCNB2 was overexpressed in multiple tumors, including gastric cancer, prostate cancer, and bladder cancer [39-42]. In this study, we found that CCNB1 is significantly highly expressed in HCC patients and is significantly associated with a poor prognosis. The inhibitory effect of Huanglian Decoction on HCC cells is mainly achieved by reducing the expression of CCNB1 protein.

Admittedly, our research also had some limitations. First of all, the paper does not carry out further research on the mechanism of CCNB1 in HCC. Moreover, it would be better if in *vivo* experiments were performed to validate our findings.

 doi:10.20944/preprints202011.0691.v1

In summary, this study demonstrates that CCNB1 is an independent prognostic indicator for HCC and was significantly associated with a worse prognosis. We also confirmed that Huanglian Decoction suppressed HCC cell growth in *vitro* by inhibiting the expression level of CCNB1 protein. Therefore, this information may help in the development of HCC treatment.

5. Funding

None applicable.

6. Competing Interests

The authors declare that there were no competing interests associated with the manuscript.

7. Availability of data and materials

The analyzed data sets generated during the study are available from the corresponding author on reasonable request.

8. Acknowledgements

Not applicable.

9. Author contributions

L.L. conceived and performed experiments and drafted the article. M.L. and H.S. conceived and performed partial experiments. T.W. and S.Y. designed the study, supervised experiments, and revised the article. All authors read and approved the final manuscript.

10. References

[1] El-Serag HB, Rudolph KL. Hepatocellular carcinoma: epidemiology and molecular carcinogenesis. Gastroenterology. 2007;132(7):2557-2576.

[2] Armengol C, Sarrias MR, Sala M. Hepatocellular carcinoma: Present and future. Carcinoma hepatocelular: presente y futuro. Med Clin (Barc). 2018;150(10):390-397.

[3] Cabrera R, Nelson DR. Review article: the management of hepatocellular carcinoma. Aliment Pharmacol Ther. 2010;31(4):461-476.

[4] Qi F, Zhao L, Zhou A, et al. The advantages of using traditional Chinese medicine as an adjunctive therapy in the whole course of cancer treatment instead of only terminal stage of cancer. Biosci Trends. 2015;9(1):16-34.

[5] Ying J, Zhang M, Qiu X, et al. The potential of herb medicines in the treatment of esophageal cancer. Biomed Pharmacother. 2018;103:381-390.

[6] Yan Z, Lai Z, Lin J. Anticancer Properties of Traditional Chinese Medicine. Comb Chem High Throughput Screen. 2017;20(5):423-429.

[7] Cheng CS, Chen J, Tan HY, et al. Scutellaria baicalensis and Cancer Treatment: Recent Progress and

Perspectives in Biomedical and Clinical Studies. Am J Chin Med. 2018;46(1):25-54.
[8] Ming-Hua C, Bao-Hua Z, Lei Y. Mechanisms of Anorexia Cancer Cachexia Syndrome and Potential Benefits of Traditional Medicine and Natural Herbs. Curr Pharm Biotechnol. 2016;17(13):1147-1152.
[9] Wang SF, Wu MY, Cai CZ, Li M, Lu JH. Autophagy modulators from traditional Chinese medicine: Mechanisms and therapeutic potentials for cancer and neurodegenerative diseases. J Ethnopharmacol.
[10] Hopkins AL. Network pharmacology: the next paradigm in drug discovery. Nat Chem Biol. 2008;4(11):682-690.
[11] Ye H, Wei J, Tang K, et al. Drug Repositioning Through Network Pharmacology. Curr Top Med Chem. 2016;16(30):3646-3656.
[12] Boezio B, Audouze K, Ducrot P, Taboureau O. Network-based Approaches in Pharmacology. Mol Inform. 2017;36(10):10.1002/minf.201700048.
[13] Liu Y, Wei L, Li XL, Pan M, Wang ZY, Dong L. Zhongguo Zhong Yao Za Zhi. 2017;42(8):1551-1556.
[14] Pan L, Li Z, Wang Y, Zhang B, Liu G, Liu J. Network pharmacology and metabolomics study on the intervention of traditional Chinese medicine Huanglian Decoction in rats with type 2 diabetes mellitus. J Ethnopharmacol. 2020;258:112842.
[15] Zhang MQ, Wilkinson B. Drug discovery beyond the 'rule-of-five'. Curr Opin Biotechnol. 2007;18(6):478-488.
[16] Matter H, Baringhaus KH, Naumann T, Klabunde T, Pirard B. Computational approaches towards the rational design of drug-like compound libraries. Comb Chem High Throughput Screen.
[17] Tao W, Xu X, Wang X, et al. Network pharmacology-based prediction of the active ingredients and potential targets of Chinese herbal Radix Curcumae formula for application to cardiovascular disease. J Ethnopharmacol. 2013;145(1):1-10.
[18] Xie W, Meng X, Zhai Y, et al. Panax Notoginseng Saponins: A Review of Its Mechanisms of Antidepressant or Anxiolytic Effects and Network Analysis on Phytochemistry and Pharmacology. Molecules. 2018;23(4):940. Published 2018 Apr 17.
[19] Kibble M, Saarinen N, Tang J, Wennerberg K, Mäkelä S, Aittokallio T. Network pharmacology applications to map the unexplored target space and therapeutic potential of natural products. Nat Prod Rep. 2015;32(8):1249-1266.
[20] Danhof M. Systems pharmacology - Towards the modeling of network interactions. Eur J Pharm Sci. 2016;94:4-14.
[21] Bortolomeazzi M, Keddar MR, Ciccarelli FD, Benedetti L. Identification of non-cancer cells from cancer transcriptomic data. Biochim Biophys Acta Gene Regul Mech. 2020;1863(6):194445.
[22] Wu X, Hasan MA, Chen JY. Pathway and network analysis in proteomics. J Theor Biol. 2014;362:44-52.
[23] Fan Z, Liu H, Xue Y, et al. Reversing cold tumors to hot: An immunoadjuvant-functionalized metal-organic framework for multimodal imaging-guided synergistic photo-immunotherapy. Bioact Mater. 2020 Aug 28;6(2):312-325.
[24] Rampersad SN. Multiple applications of Alamar Blue as an indicator of metabolic function and cellular health in cell viability bioassays. Sensors (Basel). 2012;12(9):12347-12360.
[25] Stoddart MJ. Cell viability assays: introduction. Methods Mol Biol. 2011;740:1-6.
[26] Sakata S, Enoki Y, Tomita S, et al. In vitro erythropoietin assay based on erythroid colony formation in fetal mouse liver cell culture. Br J Haematol. 1985;61(2):293-302.
[27] Heyworth CM, Dexter TM, Nicholls SE, et al. Protein kinase C activators can interact synergistically with granulocyte colony-stimulating factor or interleukin-6 to stimulate colony formation from enriched

granulocyte-macrophage colony-forming cells. Blood. 1993;81(4):894-900.
[28] Eliason JF, Odartchenko N. Colony formation by primitive hemopoietic progenitor cells in serum-free medium. Proc Natl Acad Sci U S A. 1985;82(3):775-779.
[29] Planz V, Wang J, Windbergs M. Establishment of a cell-based wound healing assay for bio-relevant testing of wound therapeutics. J Pharmacol Toxicol Methods. 2018;89:19-25.
[30] Grada A, Otero-Vinas M, Prieto-Castrillo F, Obagi Z, Falanga V. Research Techniques Made Simple: Analysis of Collective Cell Migration Using the Wound Healing Assay. J Invest Dermatol. 2017;137(2):e11-e16.
[31] Luan S, Hao R, Wei Y, et al. A microfabricated 96-well wound-healing assay. Cytometry A. 2017;91(12):1192-1199.
[32] Xu Z, Zhang F, Zhu Y, et al. Traditional Chinese medicine Ze-Qi-Tang formula inhibit growth of non-small-cell lung cancer cells through the p53 pathway. J Ethnopharmacol. 2019;234:180-188.
[33] Peng W, Zhang S, Zhang Z, et al. Jianpi Jiedu decoction, a traditional Chinese medicine formula, inhibits tumorigenesis, metastasis, and angiogenesis through the mTOR/HIF-1α/VEGF pathway. J Ethnopharmacol. 2018;224:140-148.
[34] Huang J, Guo W, Cheung F, et al. Integrating Network Pharmacology and Experimental Models to Investigate the Efficacy of Coptidis and Scutellaria Containing Huanglian Jiedu Decoction on Hepatocellular Carcinoma. Am J Chin Med. 2020;48(1):161-182.
[35] Wang N, Feng Y, Tan HY, et al. Inhibition of eukaryotic elongation factor-2 confers to tumor suppression by a herbal formulation Huanglian-Jiedu decoction in human hepatocellular carcinoma. J Ethnopharmacol. 2015;164:309-318.
[36] Zhang H, Zhang X, Li X, et al. Effect of CCNB1 silencing on cell cycle, senescence, and apoptosis through the p53 signaling pathway in pancreatic cancer. J Cell Physiol. 2018 Jan;234(1):619-631.
[37] Xie B, Wang S, Jiang N, et al. Cyclin B1/CDK1-regulated mitochondrial bioenergetics in cell cycle progression and tumor resistance. Cancer Lett. 2019 Feb 28;443:56-66.
[38] Wang Z, Fan M, Candas D, et al. Cyclin B1/Cdk1 coordinates mitochondrial respiration for cell-cycle G2/M progression. Dev Cell. 2014 Apr 28;29(2):217-32.
[39] Liu A, Zeng S, Lu X, et al. Overexpression of G2 and S phase-expressed-1 contributes to cell proliferation, migration, and invasion via regulating p53/FoxM1/CCNB1 pathway and predicts poor prognosis in bladder cancer. Int J Biol Macromol. 2019 Feb 15;123:322-334.
[40] Itkonen HM, Urbanucci A, Martin SE, Khan A, et al. High OGT activity is essential for MYC-driven proliferation of prostate cancer cells. Theranostics. 2019 Apr 12;9(8):2183-2197.
[41] Chen EB, Qin X, Peng K, et al. HnRNPR-CCNB1/CENPF axis contributes to gastric cancer proliferation and metastasis. Aging (Albany NY). 2019 Sep 16;11(18):7473-7491.
[42] Abel Dv, Abdul-Hamid O, Dijk Mv, et al. Transcription factor STOX1A promotes mitotic entry by binding to the CCNB1 promotor. PLoS One. 2012;7(1):e29769.

Preprints (www.preprints.org) | NOT PEER-REVIEWED | Posted: 27 November 2020 doi:10.20944/preprints202011.0691.v1

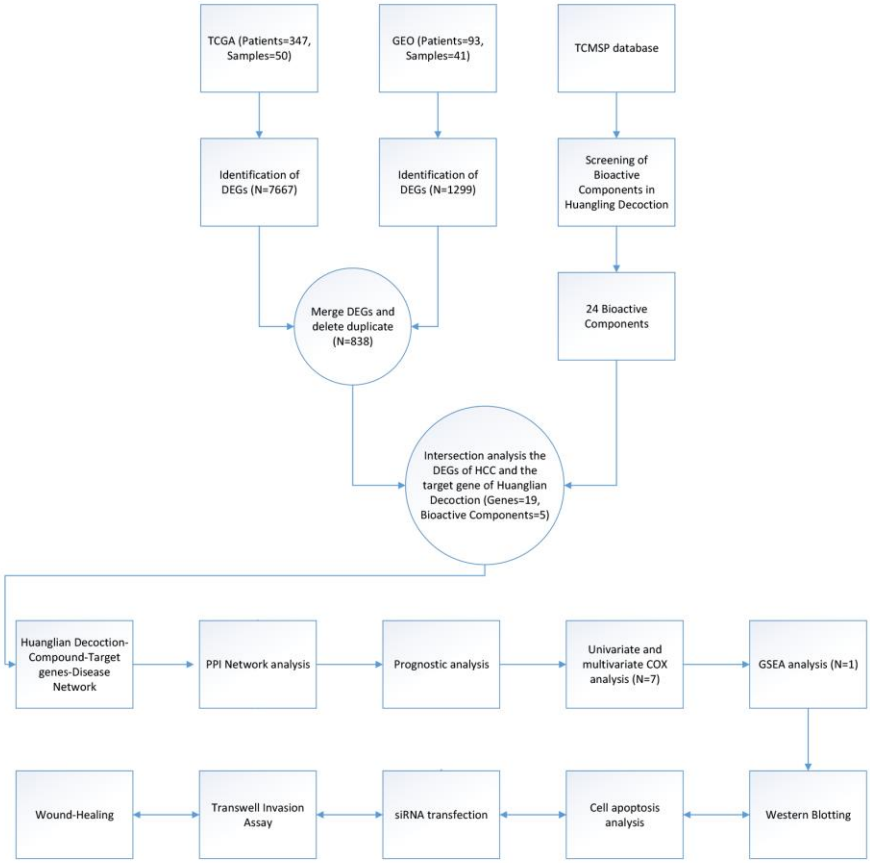

Fig. 1. Flow chart.

Preprints (www.preprints.org) | NOT PEER-REVIEWED | Posted: 27 November 2020 doi:10.20944/preprints202011.0691.v1

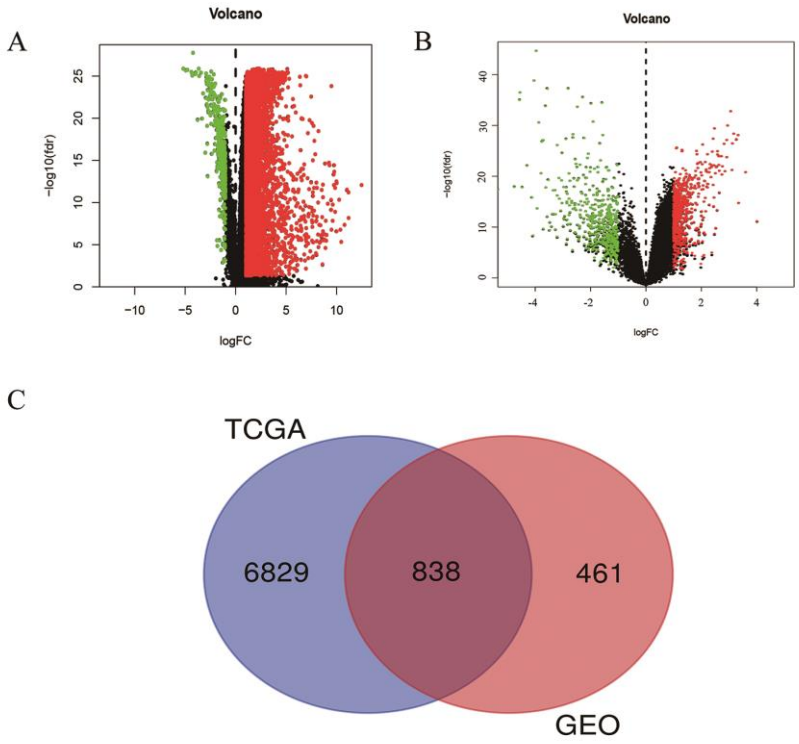

Fig. 2. Volcano and Venn diagrams of DEGs. (A) Differential gene analysis of TCGA datasets. (B) Differential gene analysis of GEO datasets. (C) The TCGA and GEO datasets show an overlap of 838 genes. Upregulated genes are marked in red; Downregulated genes are marked in light blue.

Preprints (www.preprints.org) | NOT PEER-REVIEWED | Posted: 27 November 2020 doi:10.20944/preprints202011.0691.v1

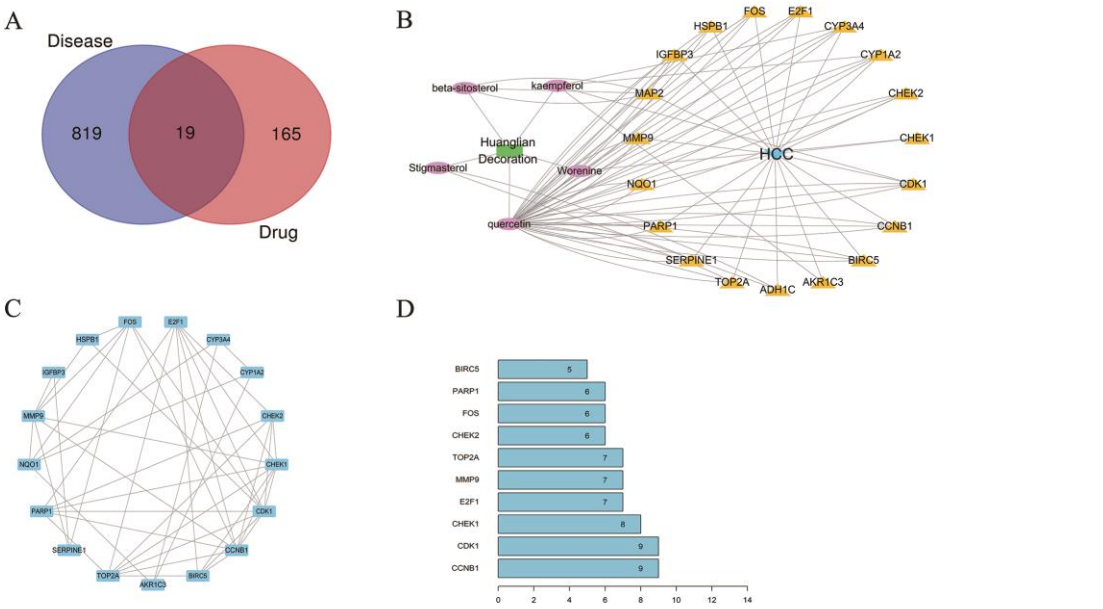

Fig. 3. Identification of key genes. (A) 19 genes overlap between DEGs of disease and drug target genes. (B) Herb-Compound network of potential bioactive constituents for Huanglian Decoction. The circles on the left are the drugs and their bioactive compounds, while the circles on the right are the target genes. (C) PPI network for target genes. The edges represent the interaction between them. (D) The top 10 genes according to the number of nodes.

Preprints (www.preprints.org) | NOT PEER-REVIEWED | Posted: 27 November 2020 doi:10.20944/preprints202011.0691.v1

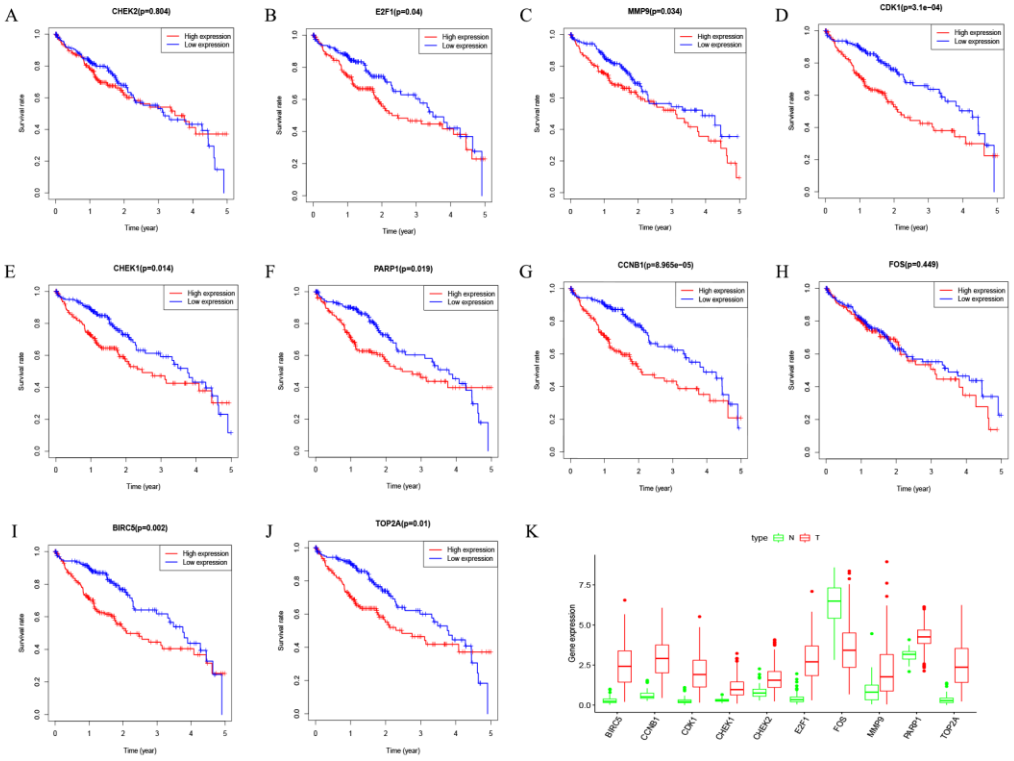

Fig. 4. Survival and expression analyses. (A) - (J) The survival analysis of the hub genes. (K) The expression analysis of the hub genes. A level of $P < 0.05$ was considered statistically significant.

Preprints (www.preprints.org) | NOT PEER-REVIEWED | Posted: 27 November 2020 doi:10.20944/preprints202011.0691.v1

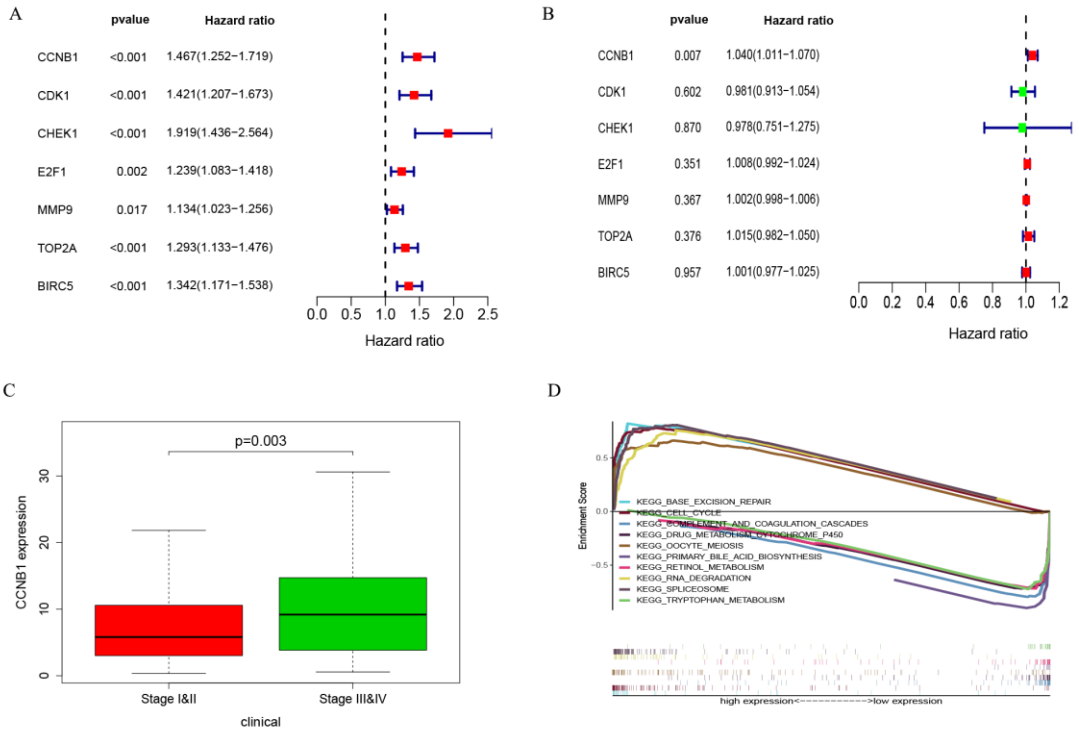

Fig. 5. Identification of key prognostic genes in HCC. (A) Univariate COX analysis. (B) Multivariate COX analysis. (C) CCNB1 found to promote tumor development. (D) The GSEA analysis reveals the biological pathways and processes associated with CCNB1.

Preprints (www.preprints.org) | NOT PEER-REVIEWED | Posted: 27 November 2020 doi:10.20944/preprints202011.0691.v1

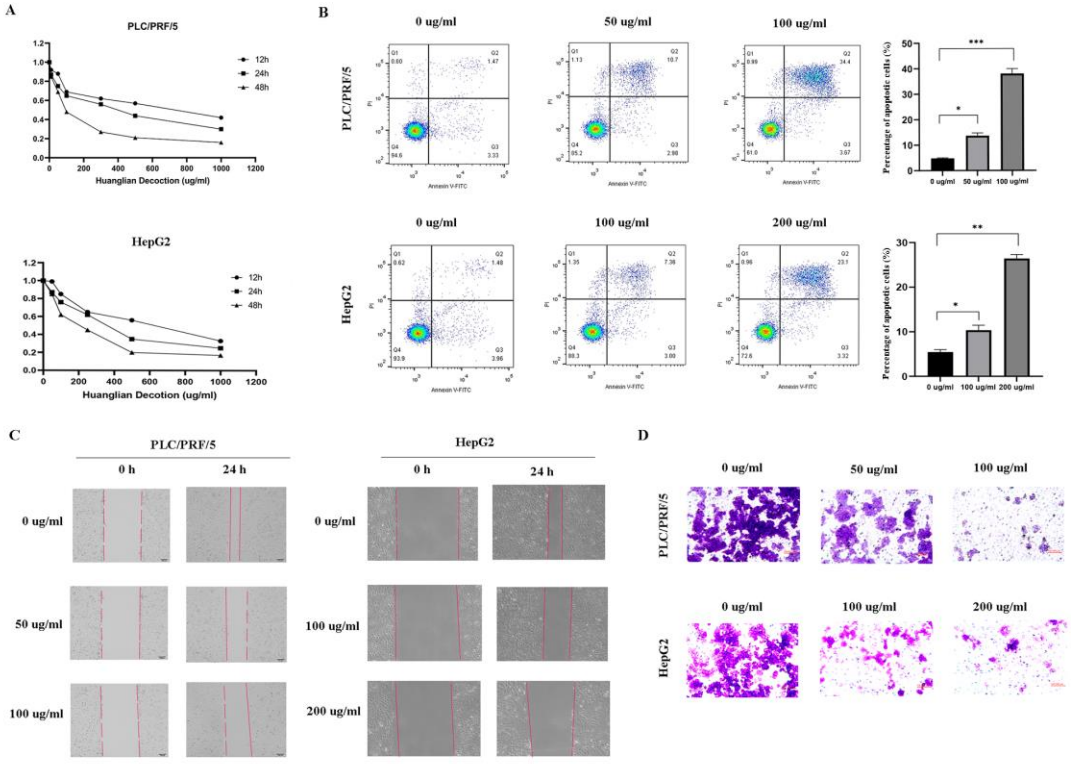

Fig. 6. Huanglian Decoction suppressed HCC cell growth in *vitro*. (A) Time- and dose-dependent effects of Huanglian Decoction treatment on the viability of both PLC/PRF/5 and HepG2 cells. (B) Huanglian Decoction can induce apoptosis of both PLC/PRF/5 and HepG2 cells. (C) Huanglian Decoction can reduce the migration activity of both PLC/PRF/5 and HepG2 cells. (D) Huanglian Decoction can reduce the invasion activity of both PLC/PRF/5 and HepG2 cells. Asterisks shows the levels of statistical significance: * = $P < 0.05$, ** = $P < 0.01$, *** = $P < 0.001$.

Preprints (www.preprints.org) | NOT PEER-REVIEWED | Posted: 27 November 2020 doi:10.20944/preprints202011.0691.v1

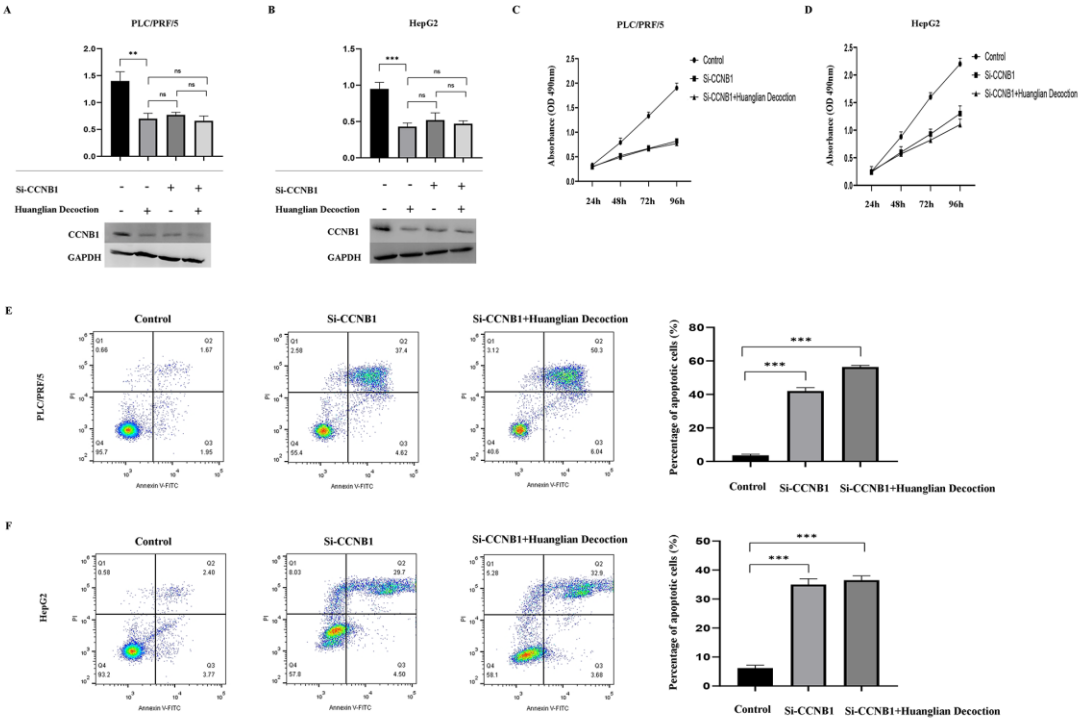

Fig. 7. Huanglian Decoction suppressed HCC cell growth in *vitro* by inhibiting the expression level of CCNB1 protein. (A and B) Huanglian Decoction can reduce the expression level of CCNB1 protein in HCC cells, but has no significant effect on the transfected cells. (C and D) At 24, 48, 72, and 96 h after transfection, cell proliferation was determined using the MTT assay. (E and F) The level of cell apoptosis increased significantly after transfection, and Huanglian Decoction exhibited no significant effect on the cells after transfection. Asterisks indicates the levels of statistical significance: * = $P < 0.05$, ** = $P < 0.01$, *** = $P < 0.001$.

Preprints (www.preprints.org) | NOT PEER-REVIEWED | Posted: 27 November 2020 doi:10.20944/preprints202011.0691.v1

T A B L E 1 GSEA analysis

NAME	ES	NES	NOM p-val	FDR q-val
KEGG_CELL_CYCLE	0.78	2.24	0.000	0.000
KEGG_BASE_EXCISION_REPAIR	0.82	2.23	0.000	0.000
KEGG_RNA_DEGRADATION	0.76	2.17	0.000	0.000
KEGG_SPLICEOSOME	0.81	2.16	0.000	0.000
KEGG_OOCYTE_MEIOSIS	0.66	2.14	0.000	0.000
KEGG_COMPLEMENT_AND_COAGULATION_CASCADES	-0.80	-2.27	0.000	0.000
KEGG_DRUG_METABOLISM_CYTOCHROME_P450	-0.72	-2.17	0.000	0.000
KEGG_RETINOL_METABOLISM	-0.73	-2.16	0.000	0.000
KEGG_PRIMARY_BILE_ACID_BIOSYNTHESIS	-0.92	-2.09	0.000	0.000
KEGG_TRYPTOPHAN_METABOLISM	0.73	-2.09	0.000	0.000

NOM p-val < 0.01 has statistically significant.

Preprints (www.preprints.org) | NOT PEER-REVIEWED | Posted: 27 November 2020 doi:10.20944/preprints202011.0691.v1

TABLE S1 Composition in Huanglian Decoction

Drug	MolId	Compounds Name
Folium Artemisiae Argyi	MOL000098	quercetin
Coptidis Rhizoma	MOL000098	quercetin
Mume Fructus	MOL000098	quercetin
Folium Artemisiae Argyi	MOL000358	beta-sitosterol
Zingiberis Rhizoma	MOL000358	beta-sitosterol
Mume Fructus	MOL000358	beta-sitosterol
Zingiberis Rhizoma	MOL000359	sitosterol
Mume Fructus	MOL000422	kaempferol
Folium Artemisiae Argyi	MOL000449	Stigmasterol
Mume Fructus	MOL000449	Stigmasterol
Coptidis Rhizoma	MOL000622	Magnograndiolide
Coptidis Rhizoma	MOL000785	palmatine
Mume Fructus	MOL000953	CLR
Folium Artemisiae Argyi	MOL001040	(2R)-5,7-dihydroxy-2-(4-hydroxyphenyl) chroman-4-one
Mume Fructus	MOL001040	(2R)-5,7-dihydroxy-2-(4-hydroxyphenyl) chroman-4-one
Coptidis Rhizoma	MOL001454	berberine
Coptidis Rhizoma	MOL001458	coptisine
Folium Artemisiae Argyi	MOL001494	Mandenol
Zingiberis Rhizoma	MOL002464	1-Monolinolein
Zingiberis Rhizoma	MOL002501	[(1S)-3-[(E)-but-2-enyl]-2-methyl-4-oxo-1-cyclopent-2-enyl](1R,3R)-3-[(E)-3-methoxy-2-methyl-3-oxoprop-1-enyl]-2,2-dimethylcyclopropane-1-carboxylate
Zingiberis Rhizoma	MOL002514	Sexangularetin
Coptidis Rhizoma	MOL002668	Worenine
Folium Artemisiae Argyi	MOL002883	Ethyl oleate (NF)
Coptidis Rhizoma	MOL002894	berberrubine
Coptidis Rhizoma	MOL002897	epiberberine
Coptidis Rhizoma	MOL002903	(R)-Canadine
Coptidis Rhizoma	MOL002904	Berlambine
Coptidis Rhizoma	MOL002907	Corchoroside A_qt
Mume Fructus	MOL005043	campest-5-en-3beta-ol
Mume Fructus	MOL008601	Methyl arachidonate

Preprints (www.preprints.org) | NOT PEER-REVIEWED | Posted: 27 November 2020 doi:10.20944/preprints202011.0691.v1

TABLE S2 Composition in Huanglian Decoction and the target gene

Drug	MolId	MolName	Target
Aiye	MOL000449	Stigmasterol	ADH1C
Wumei	MOL000449	Stigmasterol	ADH1C
Wumei	MOL000422	kaempferol	AKR1C3
Aiye	MOL000098	quercetin	BIRC5
Huanglian	MOL000098	quercetin	BIRC5
Wumei	MOL000098	quercetin	BIRC5
Aiye	MOL000098	quercetin	CCNB1
Huanglian	MOL000098	quercetin	CCNB1
Wumei	MOL000098	quercetin	CCNB1
Aiye	MOL000098	quercetin	CDK1
Huanglian	MOL000098	quercetin	CDK1
Wumei	MOL000422	kaempferol	CDK1
Wumei	MOL000098	quercetin	CDK1
Huanglian	MOL002668	Worenine	CHEK1
Aiye	MOL000098	quercetin	CHEK2
Huanglian	MOL000098	quercetin	CHEK2
Wumei	MOL000098	quercetin	CHEK2
Aiye	MOL000098	quercetin	CYP1A2
Huanglian	MOL000098	quercetin	CYP1A2
Wumei	MOL000422	kaempferol	CYP1A2
Wumei	MOL000098	quercetin	CYP1A2
Aiye	MOL000098	quercetin	CYP3A4
Huanglian	MOL000098	quercetin	CYP3A4
Wumei	MOL000422	kaempferol	CYP3A4
Wumei	MOL000098	quercetin	CYP3A4
Aiye	MOL000098	quercetin	E2F1
Huanglian	MOL000098	quercetin	E2F1
Wumei	MOL000098	quercetin	E2F1
Aiye	MOL000098	quercetin	E2F2
Huanglian	MOL000098	quercetin	E2F2
Wumei	MOL000098	quercetin	E2F2
Aiye	MOL000098	quercetin	FOS
Huanglian	MOL000098	quercetin	FOS
Wumei	MOL000098	quercetin	FOS
Aiye	MOL000098	quercetin	HSPB1
Huanglian	MOL000098	quercetin	HSPB1
Wumei	MOL000098	quercetin	HSPB1
Aiye	MOL000098	quercetin	IGFBP3
Huanglian	MOL000098	quercetin	IGFBP3
Wumei	MOL000098	quercetin	IGFBP3
Aiye	MOL000358	beta-sitosterol	MAP2
Ganjiang	MOL000358	beta-sitosterol	MAP2

Preprints (www.preprints.org) | NOT PEER-REVIEWED | Posted: 27 November 2020 doi:10.20944/preprints202011.0691.v1

Wumei	MOL000358	beta-sitosterol	MAP2
Aiye	MOL000098	quercetin	MMP9
Huanglian	MOL000098	quercetin	MMP9
Wumei	MOL000098	quercetin	MMP9
Aiye	MOL000098	quercetin	NQO1
Huanglian	MOL000098	quercetin	NQO1
Wumei	MOL000098	quercetin	NQO1
Aiye	MOL000098	quercetin	PARP1
Huanglian	MOL000098	quercetin	PARP1
Wumei	MOL000098	quercetin	PARP1
Aiye	MOL000098	quercetin	SERPINE1
Huanglian	MOL000098	quercetin	SERPINE1
Wumei	MOL000098	quercetin	SERPINE1
Aiye	MOL000098	quercetin	TOP2A
Huanglian	MOL000098	quercetin	TOP2A
Wumei	MOL000098	quercetin	TOP2A

Preprints (www.preprints.org) | NOT PEER-REVIEWED | Posted: 27 November 2020 doi:10.20944/preprints202011.0691.v1

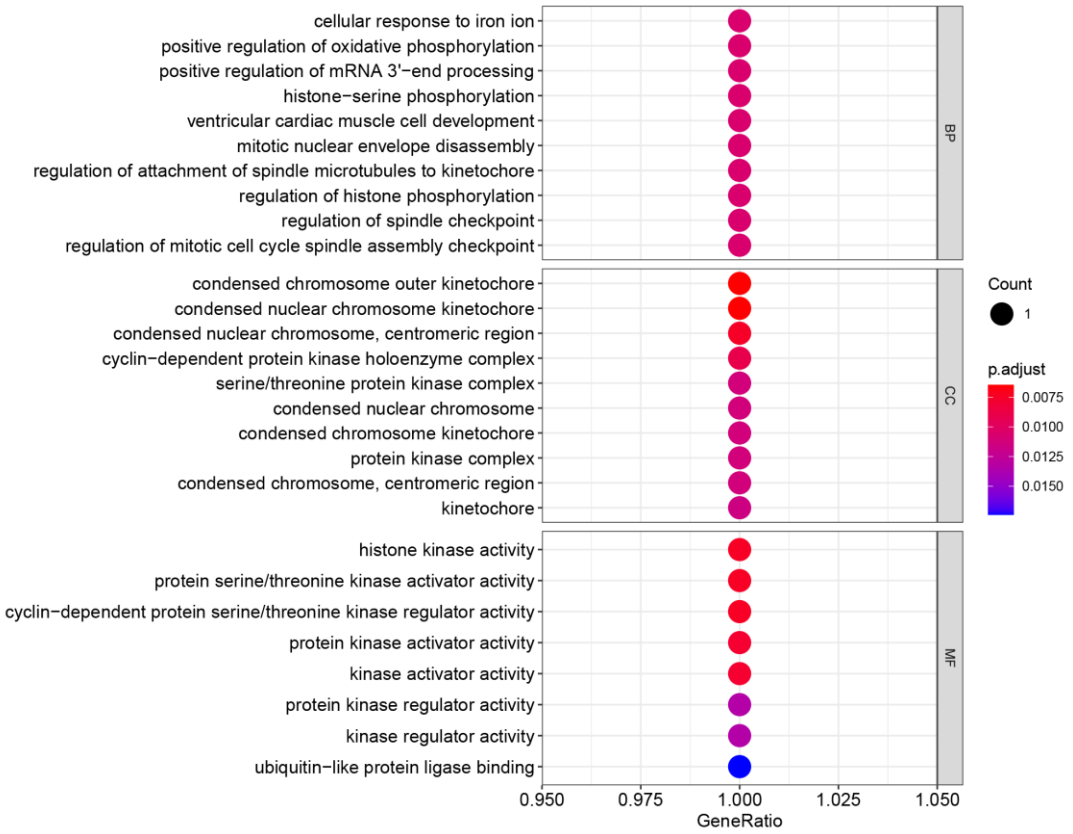

Supplementary Fig. S1. GO analysis results.

Preprints (www.preprints.org) | NOT PEER-REVIEWED | Posted: 27 November 2020 doi:10.20944/preprints202011.0691.v1

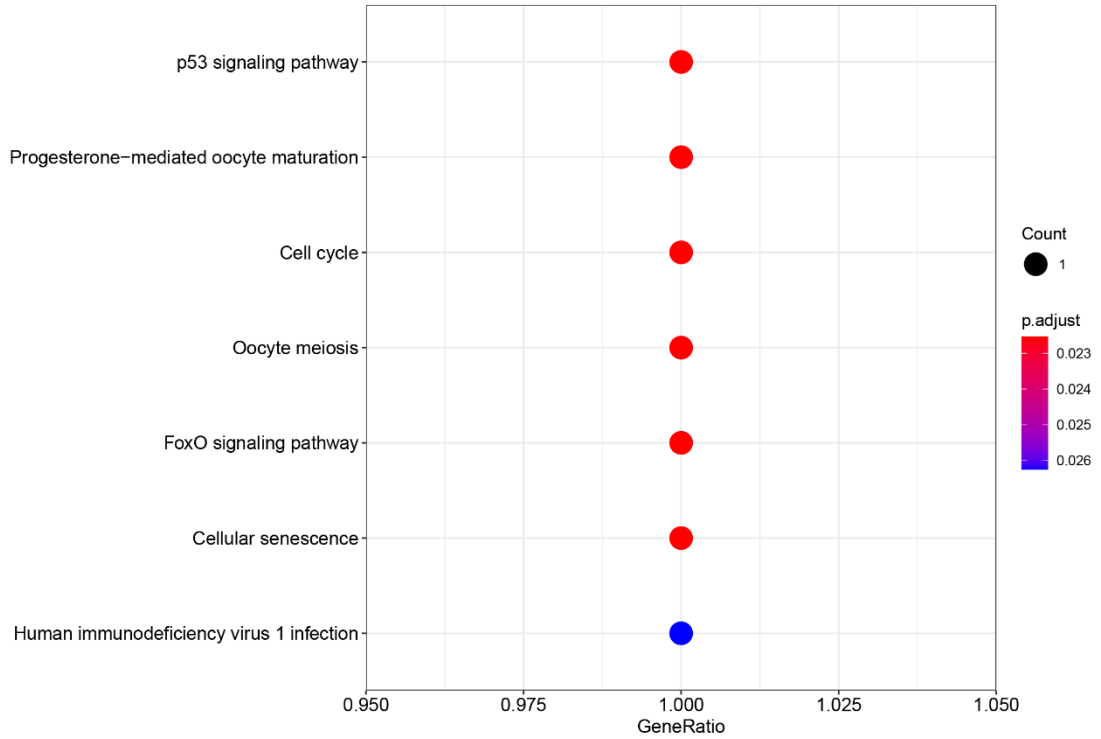

Supplementary Fig. S2. KEGG analysis results.